We are IntechOpen, the world's leading publisher of Open Access books Built by scientists, for scientists

6,900
Open access books available

185,000
International authors and editors

200M
Downloads

Our authors are among the

154
Countries delivered to

TOP 1%
most cited scientists

12.2%
Contributors from top 500 universities



WEB OF SCIENCE™

Selection of our books indexed in the Book Citation Index in Web of Science™ Core Collection (BKCI)

Interested in publishing with us?
Contact book.department@intechopen.com

Numbers displayed above are based on latest data collected.
For more information visit www.intechopen.com



Chapter

Excellency of Hydroxyapatite Composite Scaffolds for Bone Tissue Engineering

Mohammad Shariful Islam, Mohammad Abdulla-Al-Mamun, Alam Khan and Mitsugu Todo

Abstract

The hydroxyapatite [HAp, $Ca_{10}(PO_4)_6(OH)_2$] has a variety of applications in bone fillers and replacements due to its excellent bioactivity and osteoconductivity. It comprises the main inorganic component of hard tissues. Among the various approaches, a composite approach using several components like biopolymer, gelatin, collagen, and chitosan in the functionalization of scaffolds with HAp has the prospective to be an engineered biomaterial for bone tissue engineering. HAp composite scaffolds have been developed to obtain a material with different functionalities such as surface reactivity, bioactivity, mechanical strength, and capability of drug or growth factor delivery. Several techniques and processes for the synthesis and fabrication of biocompatible HAp composite scaffolds suitable for bone regeneration are addressed here. Further, this chapter described the excellences of various HAp composite scaffolds used in *in vitro* and *in vivo* experiments in bone tissue engineering.

Keywords: hydroxyapatite, scaffolds, tissue engineering, bioceramics, composite, stem cell

1. Introduction

Recently, regenerated bone grafts have drawn attention as a promising new bone grafting technology for use in tissue engineering [1]. Bone tissue engineering offers an alternative approach for repairing bone defects caused by trauma, malignancies, and congenital diseases [2]. Scaffolds are one of the key factors for bone tissue engineering. The scaffolds act as substrates by providing a temporary home for growth and proliferation of cells. The scaffolds also provide structural and mechanical support for cell growth. Therefore, scaffolds should possess sufficient mechanical strength to provide structural support and a porous structure to guide new bone tissue in-growth [1, 3, 4]. Hydroxyapatite (HAp) has been used in regenerative science dates back to the 1950s as an inert scaffold for filling of the bone defects [5]. It is a calcium phosphate bioceramic [$Ca_{10}(PO_4)_6(OH)_2$] that has widely been applied as scaffolds in bone tissue engineering because of high osteoconductivity and biocompatibility. It is a well-known bioceramic found as a major component of bone and tooth [6, 7]. HAp is one of the popular bioceramics used in bone tissue engineering because it possesses chemical structure very similar to carbonate apatite which is the major inorganic component of bone [8, 9]. HAp bioceramics have been widely

used as artificial bone substitutes because of their favorable biological properties, which include biocompatibility, bioaffinity, bioactivity, and osteoconduction [10]. HAp bioceramics contain only calcium and phosphate ions, and therefore, no adverse local or systemic toxicity has been reported in any study.

In tissue engineering, the interactions between tissue and HAp are important. Therefore, it is necessary to understand the *in vivo* host responses for HAp. Generally, the mechanism of action of a biomaterial is considered to be biocompatible, bioinert, biotolerant, and bioactive and includes bioresorbable materials. Bioactive materials form a chemical bond. The roughness and biomaterial porosity is considered to be an important factor for bonding. In this connection, HAp has displayed an ability to bond directly with the bone. It also exhibits the property of osteoinductivity [10, 11]. HAp scaffolds are very much recognized because of their osteoconduction and osteoinduction properties. Due to the provocation of the host mesenchymal stem cells, osteoinduction takes place in bone graft implantation. Therefore, these stem cells are then distinguished into bone-developing osteoblasts. Wide-ranging researches from worldwide have been accompanied several researches to recognize the osteoinduction potential of HAp over the past numerous years. As a result, through a number of independent studies in several hosts such as dogs, goats, and baboons osteoinduction has been finally detected [11–14]. In relation to the previous development, recently, comprehensive studies have been performed to construct biomimetic scaffolds materials for bone tissue engineering utilizations. Three-dimensional structure of these biomaterials is very much necessary for proper functioning. Few excellent properties of these scaffolds such as a high volume of open and interconnected pores, a bioresorbable scaffold with controlled resorption, appropriate mechanical properties, biocompatibility, and bioactivity are highly recommended in bone tissue engineering [15].

Various permeable scaffolds can be assembled by using both bioactive ceramics and biocompatible polymers for the application in bone tissue engineering [1]. The bioactivity of graft substitutes is mostly governed by the degree of porosity of the fabricated biomaterials, which controls the rate of bone regeneration, local environment, and equilibrium of new bone at the repair site. Therefore, the osteoconductivity of the inductivity potential of the bone graft is synergistically promoted by the pore interconnectivity, geometry, topography, and porosity modulate osteogenesis of the fabricated scaffolds [16–18]. Bioactive ceramics have a chemical composition resembling that of natural bone, allowing osteogenesis and providing bony contact and bonds with host bone [6, 19]. HAp is a typical bioceramic clinically used as a bone substitute, and it has also been used as scaffold materials in bone tissue engineering owing to its bioactivity, biocompatibility, and osteoconductivity. However, the low strength and toughness of HAp has limited its wide application in orthopedic implants [20]. The main reason for these low mechanical properties is thought to be the decomposition of HAp into different calcium phosphate phases, such as tricalcium phosphate (TCP) and even tetracalcium phosphate (TTCP) [21]. Therefore, the mechanical properties of the HAp porous scaffold must be enhanced to use effectively in load-bearing compartments and tissue engineering applications. Various kinds of natural polymers, synthetic polymers (chitosan), protein (collagen), and bioceramics have been used along with HAp to develop composite porous scaffolds for bone tissue engineering in recent years.

2. Synthesis and fabrication processes

Scaffold fabricated by various methods acts as a substrate to stimulate cell adhesion, maintenance of differentiated cell function without hampering proliferation. It is also a template to establish and direct the growth of cells and help in

the construction of extracellular matrix (ECM) [22]. Therefore, a biodegradable scaffold serves as a temporary skeleton in bone tissue engineering. Generally, when such scaffolds are inserted into the sites of faulty or lost bone to support and stimulate bone tissue regeneration, they gradually degrades and is replaced by new bone tissue [23–25]. The use of HAp as a scaffold material has been introduced in bone tissue engineering mainly due to its unique properties and similarity with bone components. The low strength and toughness of HAp has limited its wide application in bone tissue engineering. Therefore, improved mechanical properties of the HAp porous scaffolds are required for the extensive range of applications and effective utilization in load-bearing compartments [1]. To overcome the brittleness of HAp porous body, biodegradable synthetic polymers such as poly (lactic co-glycolic acid) (PLGA), para-Methoxy-N-methylamphetamine (PMMA), poly(L-lactic acid) PLLA, and poly(ε-caprolactone) PCL are used as composites [26–29]. Even some attempts have been made to introduce bioceramics into polymer-based scaffolds or to combine synthetic polymers with natural polymers to enhance their biological capacity [30]. Recently, several studies are focusing on the development of HAp-COL and HAp-COL/HAp composite scaffolds or HA-CNT nanocomposites with improved mechanical properties [31, 32]. HAp-COL and HAp-COL/HAp composite scaffolds or HA-CNT nanocomposites for orthopedic implants are synthesizing through template method, plasma spraying, laser surface alloying, electrophoretic deposition, and aerosol deposition [31, 33–37]. In addition to conventional sintering and hot isostatic pressing, spark plasma sintering (SPS) has also been employed to fabricate freestanding HA-CNT composites [38–41]. HAp-COL and HAp-COL/HAp composite scaffolds are also fabricated in a specific freeze-drying procedure [31].

2.1 Synthesis of HAp porous scaffolds by the template method

A template method (using polyurethane foam [PU]) was applied to prepare HAp porous scaffolds from HAp slurry. The HAp slurry was synthesized from HAp nanopowder and a 5 wt% solution of polyvinyl alcohol (PVA) (Wako Pure Chemical Industries, Ltd.). The HAp slurry was prepared by mixing the HAp powder and PVA solution at a mixing ratio of 1:1 (1 g of HAp to 1 ml of PVA) using a centrifuge mixing machine (Imoto Co, Ltd.). The machine was kneading for 10 minutes and degassing (removal of gas bubbles) for 8 minutes to obtain the best outcome. A PU sponge sheet (HR-30, Bridgestone) was cut into cubic templates with dimensions of 10 × 10 × 10 mm. These cubes were then immersed into the ready HAp slurry. To escape blockage of the pores by the slurry, the additional slurry was removed by pressing the cubes at compression ratios of 50, 75, and 95%. To eliminate water content and to attach the HAp powders to the surface of the sponge framework, the cubes were then dried out at room temperature for 24 hours. The dried cubes were then calcined at 400°C for 6 hours and further sintered at 1000, 1100, or 1200°C for 3 hours. The heating rate was set to 10°C/minute. The solidified samples were termed "pure HAp scaffolds" thereafter. The sintering process is illustrated schematically in **Figure 1(a)** [1].

2.2 Fabrication of HAp porous scaffolds with collagen and HAp particles

In a collagen-1 solution prepared, pure HAp scaffolds were dipped (Nippon Meat Packers Inc., Osaka, Japan) and then it was vacuumed for at least 30 minutes to eliminate the excess air. To synthesize HAp scaffolds with collagen coating, firstly, the surplus collagen solution was removed manually by pipette, and then the samples were dried at room temperature for at least 48 hours. On the other hand, a milk-like slime of HAp particles was formulated by mixing it accurately with the collagen-1 solution

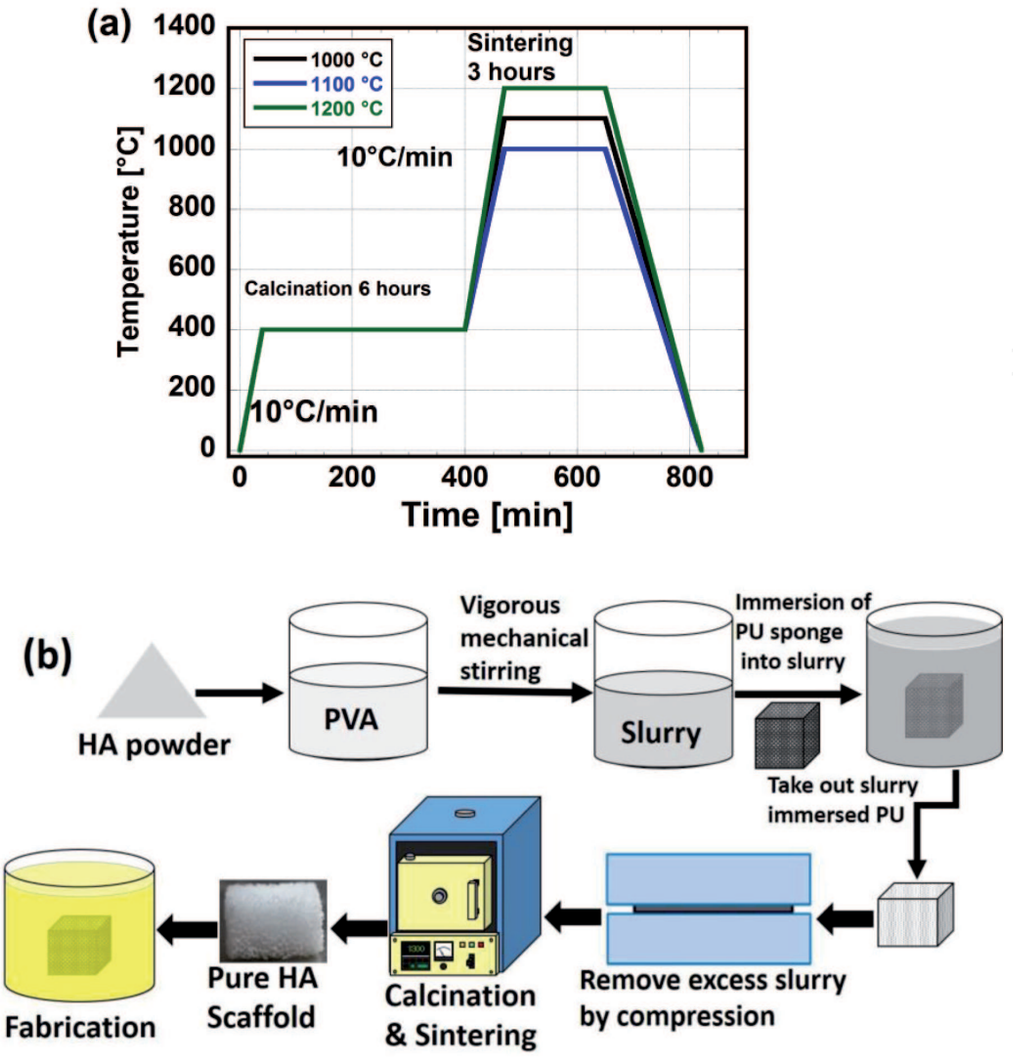


Figure 1.
Schematic of the (a) sintering processes and (b) synthesis to the fabrication of HAp porous composite scaffolds [1].

(1:9) at 30°C and stirred continuously by a magnetic stirrer. To fabricate HAp scaffolds with collagen-HAp coating, the prepared slime was then poured over the pure HAp scaffolds. After that, the additional slime was removed and the scaffolds were dried out for at least 48 hours to get fabricate HAp scaffolds. The two distinct types of fabricated composite scaffolds were thereafter termed as "HAp-COL" and "HAp-COL/HAp particle-coated scaffolds," respectively. The detail fabrication processes of the HAp-COL and HAp-COL/HAp scaffolds are illustrated schematically here in **Figure 1(b)** [1]. Further, a specific freeze-drying procedure was applied to fabricate coated HAp scaffolds form both types. The pure HAp porous composite scaffolds were frozen at −20°C for 24 hours and then freeze-dried at −50°C for 24 hours. These samples were termed "HAp-Collagen or HAp-Collagen/HAp particles two-phase scaffolds" [31].

2.3 Fabrication of HAp composite by Nd-YAG laser

HAp composite scaffolds were fabricated by a unique process where HAp powders were coated on titanium substrates at low temperature, and this coating/substrate interfacing was enhanced by a laser surface engineering. In this technology, Nd-YAG laser was transmitted to HAp powders and the laser power was absorbed by titanium substrate to produce a thin layer of the molten region. Finally, in this procedure, HAp powders were kept at low temperature before they were entrapped in the metallic layer during coating [35].

2.4 Fabrication of HAp composite by electrophoretic deposition (EPD)

Usually, various bioactive ceramics like HAp are coated containing carbon nanotubes on metallic substrates through electrophoretic deposition. The EPD technique is described by Sing et al.. Using EPD, a variety of potentially bioactive ceramic coatings constructed on combinations of either HAp or titanium oxide nanoparticles with carbon nanotubes (CNTs) have been deposited on metallic substrates. Further, sol-gel-derived ultrafine HAp powders (10–70 nm) were dispersed in multi-wall nanotube-containing ethanol suspensions maintained at pH = ~3.5 and successfully coated onto Ti alloy wires at 20 V for 1–3 minutes. Commercially available TiO2 nanopowders and surface-treated CNTs in aqueous suspensions were co-deposited on stainless steel planar substrates for TiO2/CNT coatings. A field strength of 20 V/cm and a deposition time of 4 minutes were used in this process to work at pH = 5 [36].

2.5 Fabrication of HAp composite by aerosol deposition

Hahn et al. developed an aerosol deposition technique to fabricate HAp-carbon nanotube (CNT) composite coatings on Ti plate. Through this aerosol deposition technique, authors fabricating HAp-CNT powders composites for biomedical applications. For the deposition process, HAp-CNT powder mixtures with CNT contents of 1 and 3 wt.% were used. Dense coatings with a thickness of 5 μm were fabricated, irrespective of the content of CNTs. The propagation and alkaline phosphatase (ALP) activity of MC3T3-E1 pre-osteoblast cells grown on the HAp-CNT composite coatings was estimated. A higher propagation and alkaline phosphatase (ALP) activity of MC3T3-E1 pre-osteoblast cells grown on the fabricated HAp-CNT composite coatings was detected than those on the bare Ti and pure HAp coating. It was also found that by increasing the CNT content of the composite materials, an enhanced ALP activity of the composite coatings was obtained. Therefore, the findings suggested that for the improvement both the mechanical and biological performances of HAp coatings, CNTs would be an effective fortifying agent [37].

2.6 Fabrication of HAp composite by in situ chemical vapor deposition

Li et al. described a novel process to fabricate carbon nanotubes (CNTs) (Fe)/HAp composite. By this novel process (CNTs), (Fe)/HAp composite was successfully prepared where CNTs homogeneously dispersed. In this procedure, at first Fe_2O_3/HAp precursor was produced and then calcined in an atmosphere of N_2 gas. The reduction reaction was done in the presence of hydrogen of the Fe_2O_3/HAp precursor to yield Fe/HAp catalyst, and finally, in situ synthesis of nanotubes by chemical vapor deposition over Fe/HAp catalyst was performed. To yield CNTs (Fe)/HAp bulk composites, these outstanding CNTs (Fe)/HAp composite powder was utilized. These CNTs (Fe)/HAp bulk composites further pressed and sintered to produce CNTs (Fe)/HAp nanocomposites. It was analyzed that the CNTs distributed homogenously and bonded strongly with the HAp matrix [39].

2.7 Fabrication of HAp composite by poly(ε-caprolactone) (PCL) and poly(L-lactide) (PLLA)

PCL pallets with the molecular formula $(CH2)_5CO_2$, molecular weight (Mw) of 10^5g.mol^{-1}, glass transition temperature Tg = −62.62°C, and melting point Tm = 65.4°C (Celgreen PH7, Daicel Chemistry Industries Co., Ltd.) were dissolved

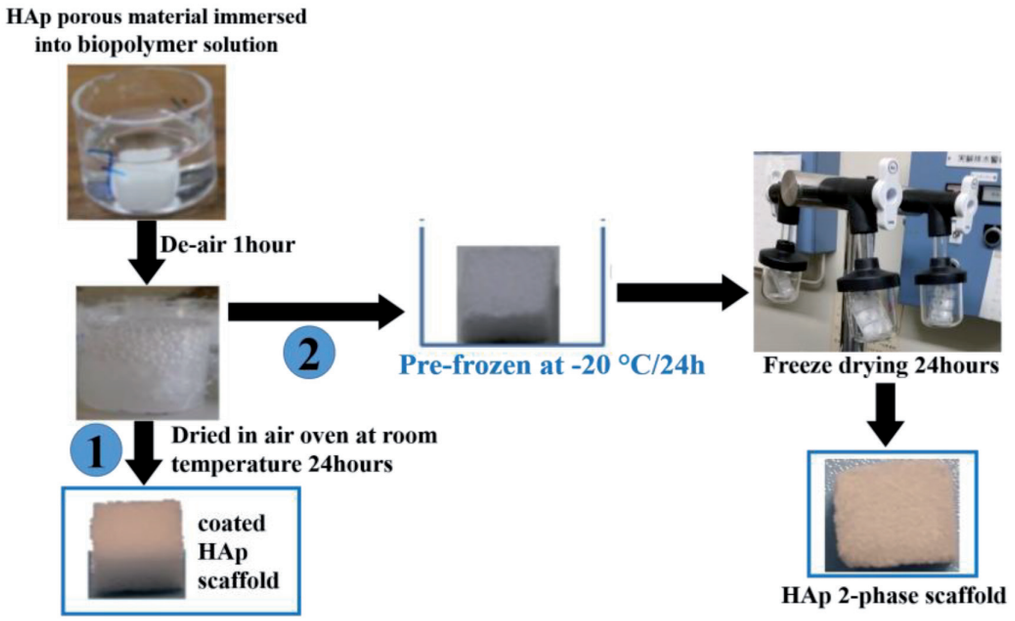


Figure 2.
Schematic of biopolymer-reinforced HAp porous materials.

in 1,4 dioxane (Kishida Chemical Co., Ltd., Osaka, Japan) to get the solution with a concentration of 1, 3, 5, 7 and 10 wt% by stirring at 60°C for 2 hours. HAp porous scaffolds were dipped into the solution, and it was then vacuumed for 1 hour to eliminate the air. For drying of these scaffolds, two different conditions were applied. The drenched HAp porous scaffolds were taken out from the PCL solution and then dried in an air oven at room temperature for 24 hours in the first drying process. These specimens were named as "HAp/PCL-coated scaffolds." On the other hand, in the second drying process, the freeze-drying procedure was employed to obtain a two-phase porous construction. After excess PCL solution was removed from the soaked HAp porous materials, the samples were frozen at −20°C for 24 hours and then freeze-dried at −50°C for 24 hours. These specimens were named as "HAp/PCL 2-phase scaffolds." The summary of the reinforcement process is shown in **Figure 2** [42].

3. Excellences in bone tissue engineering

The scaffolds act as a temporary substitute in bone tissue engineering and the interest of researchers in it as it permits mechanical support until the tissue has regenerated and remodeled itself naturally. It is well established that biopolymers such as collagen [43], chitosan [44], and hyaluronic acid [45]; biodegradable synthetic polymers such as poly(L-lactic acid) [46], poly(ε-caprolactone) [47], and polyglycolic acid (PGA) [48]; and bioactive ceramics such as hydroxyapatite [49], α-tricalcium phosphates [50], and β-tricalcium phosphates (β-TCP) [51] are used as the raw materials for the preparation of the scaffolds suitable for tissue engineering. These materials have been independently used to develop scaffolds, but composite materials have also been considered as ideal materials having mechanical stability, biocompatibility, cell proliferation, and easy proccessability [52–55]. However, HAp grows interested in scientists and researchers due to its mechanical and biological response and its efficiency in repairing a hard tissue defect in the composite state. This section will summarize the excellence of different HAp composite scaffolds for bone substitutes and hard tissue repair.

3.1 *In vitro* experiments using HAp composite scaffolds

Phanny (in our lab) conducted a study using HAp/PCL-coated scaffold and HAp/PCL two-phase scaffold to investigate the mechanical properties variation, biocompatibility, and differentiation efficiency within 4 weeks of cell culture in a standard medium and osteoblast differentiation medium [42]. Human mesenchymal stem cells (hMSCs) were seeded in both types of scaffold for 1–4 weeks with an α-minimum essential medium eagle with L-glutamine and phenol red (MEMα) for the growth and with osteoblast differentiation medium for cellular differentiation. The author reported that both HAp/PCL-coated scaffold (**Figure 3**, left) and HAp/PCL two-phase scaffolds were biocompatible where hMSCs have grown and proliferated rapidly (**Figure 3**, right). The level of p-nitrophenol obtained via ALP assay of both types of scaffolds are almost the same because the cells tended to proliferate in standard medium rather than differentiation. The cells cultured in osteoblast differentiation medium were able to differentiate into an osteoblastic lineage with an increasing level of p-nitrophenol and density of ARS staining. It was also found that specimens without cell seeding continuously decreased in both elastic modulus and compressive strength in both standard medium and osteoblast differentiation medium and remained lower than that of specimens with cell culture.

Therefore, it was concluded that the ability to allow cells to grow, proliferate, differentiate, and maintain mechanical properties of HAp/PCL-coated and two-phase scaffolds are a high potential candidate for bone tissue engineering applications [42].

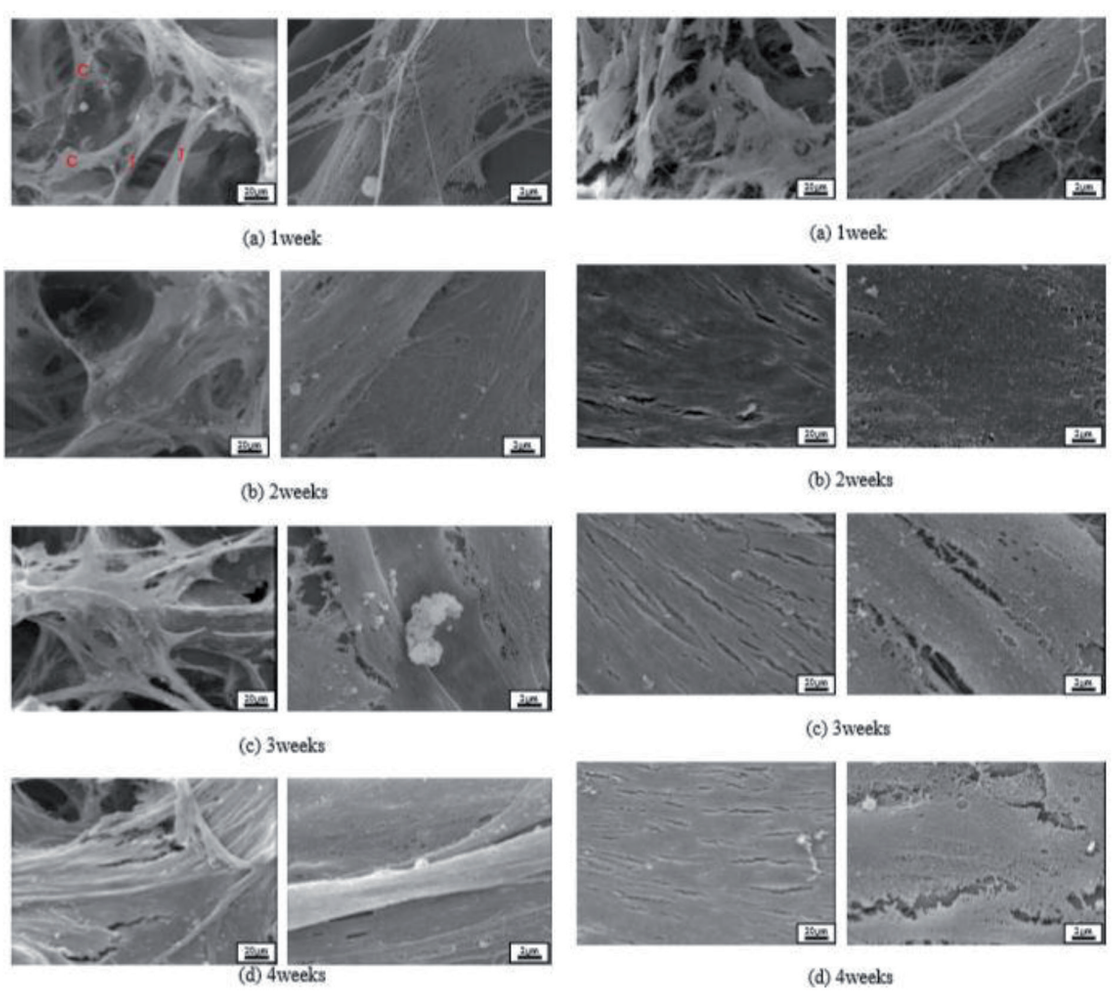


Figure 3.
FE-SEM images of the morphology of cell growth on HAp/PCL-coated (left) and HAp/PCL two-phase scaffolds (right).

It was reported in our previous study that hMSCs could be successfully cultured over HAp-COL and HAp-COL/HAp scaffolds. It was confirmed from that evaluation that the scaffolds exhibited the best performance in terms of mechanical properties at a 50% compressive ratio. **Figure 4** represents the FE-SEM micrographs of the surface regions of composite scaffolds with hMSCs [1]. In this figure, hMSCs's adhesion and proliferation behaviors up to 7 days of culturing were observed on the surfaces. The FE-SEM micrographs of hMSCs cultivated over the fabricated composite scaffolds of HAp-COL and HAp-COL/HAp sintered at 1000, 1100, and 1200°C are shown in figures (a), (c), and (e), and (b), (d), and (f), respectively. Most cells adhered tightly to the surface and were well disseminated. These results indicated that the composite scaffolds had favorable bioactivity for the promotion of cell adhesion and proliferation far excelling than that of pure HAp scaffolds. The effects of the compressive ratio and sintering temperature on cell-scaffold interactions were evaluated through a cell proliferation assay using a cell-counting kit up to 14 days of culture.

The growth performance of hMSCs over the constructed porous composite scaffolds is exhibited in **Figure 5**. Primarily, 1×10^4 cells were seeded on the fabricated porous composite scaffolds. After the cells seeding well, the cell proliferation

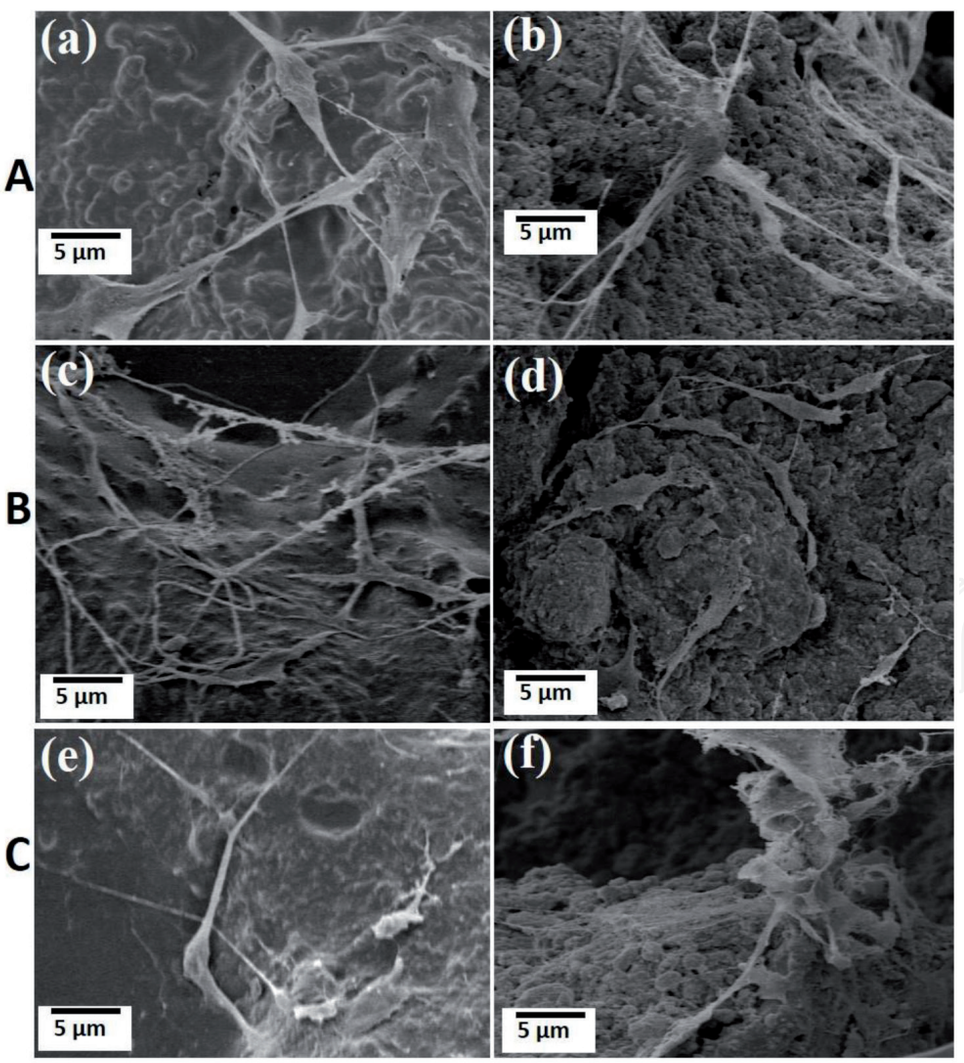


Figure 4.
The FE-SEM images of 7 days culture period of hMSCs over HAp-COL and HAp-COL/HAp porous composite scaffolds fabricated at a 50% compressive ratio and sintered at (A) 1000C, (B) 1100°C, and (C) 1200°C. the FE-SEM images HAp-COL and HAp-COL/HAp porous composite scaffolds are represented by (a), (c), and (e) and (b), (d), and (f) at sintering temperature 1000°C, 1100°C, and 1200°C, respectively [1].

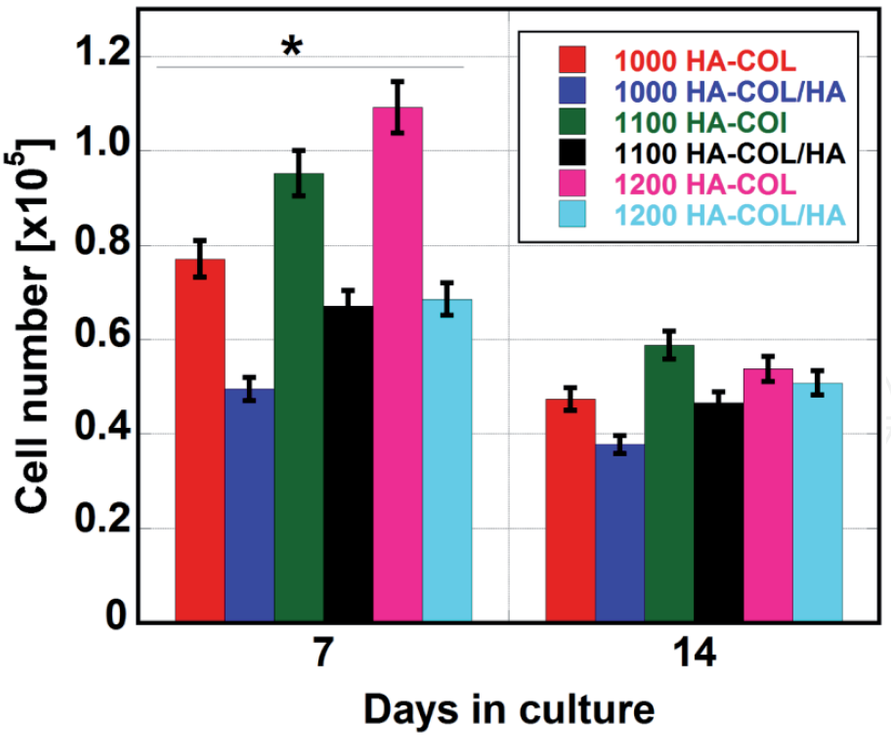


Figure 5.
*The proliferation of hMSCs in HAp-COL and HAp-COL/HAp composite scaffolds fabricated at a 50% compressive ratio and sintered at 1000, 1100, and 1200°C with up to 14 days of culture. Each set of data represents the mean ± SD, n = 6, *p < 0.05 [1].*

behavior was recorded at 7 and 14 days of culture. It was noteworthy that the cell number increased until 7 days of culture for all types of scaffolds, while cell multiplication declined as the culturing days continued. The growth performance of hMSCs over the HAp-COL scaffolds sintered at 1000, 1100, and 1200°C displayed distinctive trend over their counterparts [1].

Wahl and Czernuszka summarized and compared a few excellent reports of *in vitro* experiments using HAp composite scaffolds and are listed here in **Table 1** [56].

3.2 *In vivo* experiments using HAp composite scaffolds

Cai et al. fabricated coral hydroxyapatite (CHAp) as a cuboid of 5 mm × 5 mm × 10 mm with an inclined groove. In this study, the prepared CHAp biomaterials was highly porous (porosity: 30–70%) with a fully interconnected pore with an average pore diameter of 100–600 μm. Here, the induced BMSCs

Composites	Cell culturing or implantation	Period (new tissue formed)
HA-Collagen (Du et al.) [57]	Bone extract wrapped around composite osteogenic cells	21 days (mineralized bone)
HA-Collagen (Clarke et al.) [58]	Human-derived bone cell culture	32 days (connective tissue and mineralized bone)
HA-Collagen (Wu et al.) [59]	Osteoblasts from rat calvaria	21 days (mineralized bone)
HA-Collagen (Wang et al.) [60]	Chondrocytes in a closed chamber	49 days (cartilage)
HA-Collagen-Elastin (Rovira et al.) [61]	Osteoblasts from trabecular bone	15 days (mineralized bone)

Table 1.
In vitro *experiments in bone tissue engineering using different HAp composites.*

were seeded on sterilized CHAp scaffold by a concentration of 20 × 10^6 cells/ml (200 ± 17 μL/scaffold, about 4 × 10^6 cells/scaffold) and were 3D cultured for 1 week before implantation. The growth behavior of BMSCs on the CHAp scaffold was assessed by using a scanning electron microscope and confocal laser electronic microscope [62]. The authors described an effective methodology to generate bone tissue and healing bone defect in ectopic and orthotopic sites. In this methodology, a tissue-engineered bone flap with a vascular pedicle of saphenous arteriovenous with an organized vascular network was observed after 4 weeks of implantation and followed by a successful repair of the fibular defect in beagle dogs (**Figure 6**).

Engineered bone formation in ectopic and orthotopic sites after implantation of 9 months over four CHAp scaffold groups were evaluated by CT (computed tomography) analysis. The stimuluses of vascularization and micro-environment on tissue-engineered bone were quantitatively analyzed by the comparison of bone formation and scaffold degradation between different groups **(Figure** 7). The results indicated that in the first 3 months, vascularization improved engineered bone formation by 2 times of non-vascular group and bone defect micro-environment improved it by 3 times the ectopic group, and the CHAp scaffold degradation was enhanced as well [62]. In the VSC group, the HE staining of decalcified paraffin sections after 3 months embedding exhibited that there was a minor volume of bone-like tissue developed at the surface of the CHAp scaffold (**Figure 7(B)**). **Figure 7(C)** and **(D)** indicates the gradual improvement of engineered bone tissue after 6 months and a well-developed Haversian system with little residual scaffold remaining after 9 months, respectively. In the SC group, after 3 months of implantation, only the osteoid was shown and until 6 months of implantation, there was no significant bone formation, but after 9 months of implantation, engineered bone tissue enlarged with much residual scaffold (**Figure 7(E)–(H)**). **Figure 7(I)–(P)** denotes the gradual degradation of the CHAp scaffolds without bone formation in both VS and S groups, the pores of the majority of CHAp scaffold fill with fibrous connective tissue and a large number of inflammatory cells. Moreover, more typical vascular structures and less inflammatory cells were seen in the VS group than that in the S group (**Figure 7L** and **P**).

In another study, Kikuchi et al. (2001) fabricated a biodegradable hydroxyapatite/collagen (HAp/Col) nanocomposite [63]. In this method, through the lyophilization of the precipitate of HAp/Col composites, HAp/Col powder was formulated. About 0.5 g of the prepared HAp/Col powder was well mixed with 3 ml of 0.9% NaCl solution (Wako, Japan) and 35 Al of 5 M CaCO3 (Wako). In a 0.9% NaCl

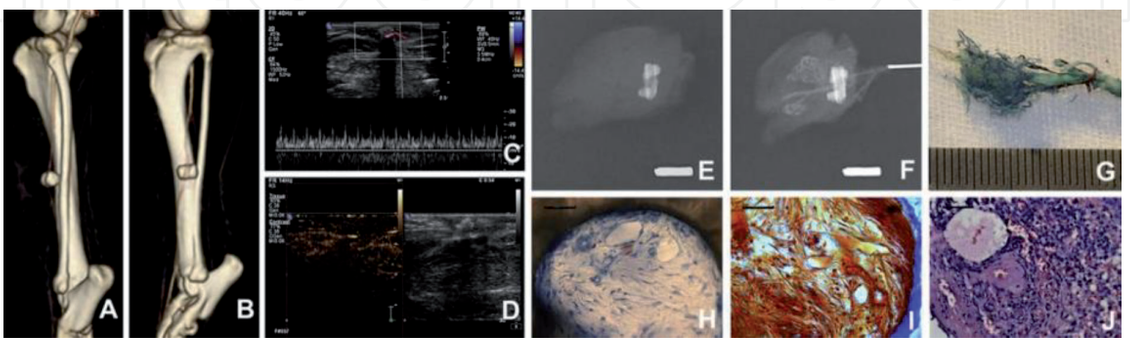


Figure 6.
Representation of the vascularization over MSC coral hydroxyapatite scaffold using cell-CHA constructs at 4 weeks post-implantation. Here, (A) and (B) represent CT angiography and (C) and (D) indicate ultrasonic inspection. Further, (E) and (F) indicate X-ray before and after vascular corrosion cast and (G) represent vascular corrosion cast. HE and Masson's trichrome staining of cell-CHA constructs in undecalcification sections and decalcification sections is indicated by (H), (I), and (J), respectively. Scale bars: 10 mm (F), (G), 50 mm (H)–(J) [62].

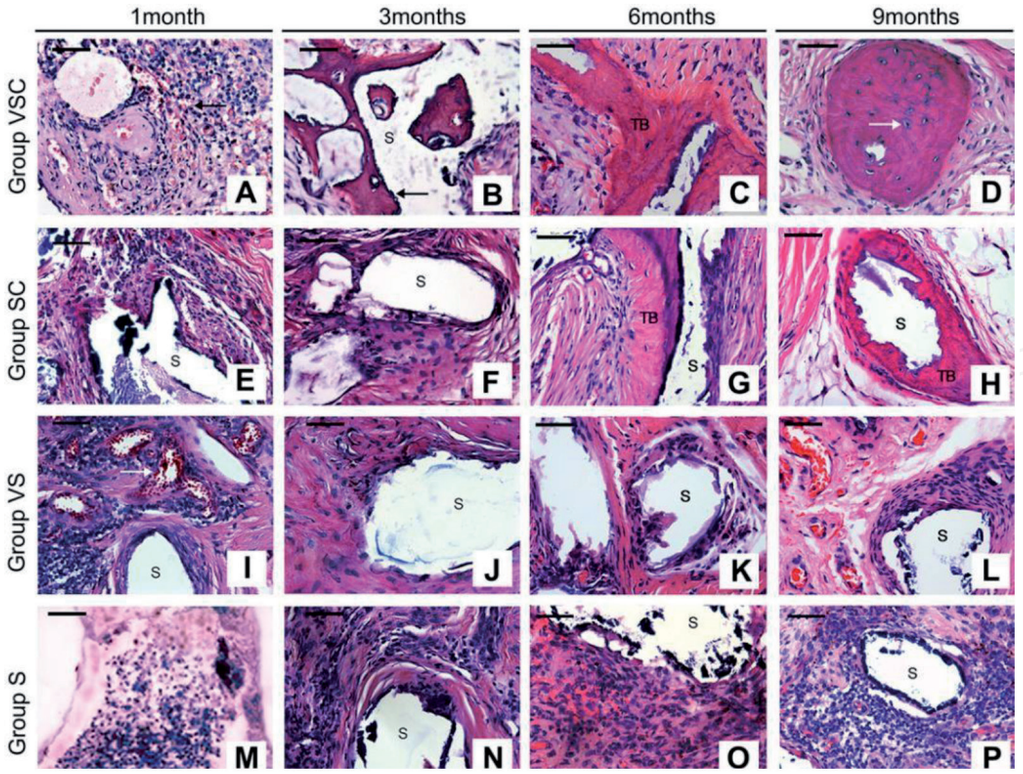


Figure 7.
Histological observation of different CHAp-scaffold constructs implanted into spatium intramuscular of the hind limb at 1, 3, 6, and 9 months post-implantation (HE staining; S, CHA scaffold; TB, tissue-engineered bone). Scale bars: 50 mm. Here, HE staining of decalcified paraffin sections is showed. In VSC group, bone-like tissue formation at the surface of the CHA scaffold after 1 and 3 months implantation are indicated by plate (A) and (B), respectively; gradual increase of engineered bone tissue after 6 months and visible well-developed Haversian system after 9 months implantation are indicated by plate (C) and (D), respectively. In SC group, visible osteoid after 3 months, no significant bone formation until 6 months and engineered bone tissue increased with much residual scaffold remaining after 9 months implantation are represented by (E), (F), (G), and (H), respectively. Filling the pores of the CHA scaffolds in both VS and S groups with fibrous connective tissue and a large number of inflammatory cells indicated by (I–P).

solution, 1.5 ml of 3% sodium alginate (Wako) was added, dissolved, and mixed. D-gluconic acid lactone (60 mg, Sigma, USA) was added to the HAp/Col-alginate mixture to initiate gelation, and the mixture was injected into a mold and left for 45 minutes at room temperature. The composite has a bone-like nanostructure; the length of the HAp crystals is up to 50 nm. The authors investigated the capability of HAp/Col-alginate as a bone filler in the rat femur and as a carrier of BMP using an ectopic bone formation model (**Figure 8**). Vigorous bone growth around the fabricated scaffolds and tissue invasion into these scaffolds was observed during the experiment. A comparison was made between those observed for simple alginate and porous HAp. Furthermore, HAp/Col-alginate was investigated as a carrier of recombinant human bone morphogenetic protein 2 (rh-BMP2). It was revealed that bone formation throughout the implant 5 weeks after implantation without obvious deformation of the material was obtained by using the HAp/Col-alginate (20 μl) with the rh-BMP2 (100 μg/ml, 15 μl), whereas bone development was detected only in a part of a squashed collagen sponge [64]. In **Figure 8 (A–C)**, prominent bone formation of the HAp/Col-alginate treated with the 100 μg/ml BMP solution was remarkably extended throughout almost the whole implant, and bone marrow-like tissue also developed. It was noticed that the implants shrank when there was no bone formation. Further, it was observed that ectopic bone formation was obtained using collagen sponge treated with the 100 μg/ml of rh-BMP2 solution, but new bone had not extended all through the implant even after 5 weeks (**Figure 8(D)**) [64].

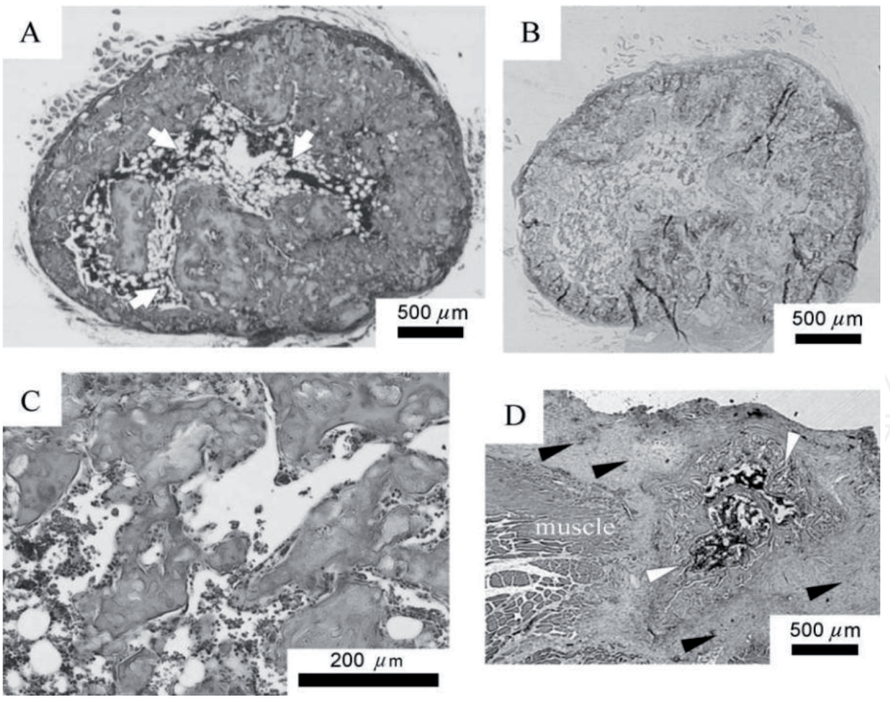


Figure 8.
BMP2 (100 μg/ml) induced ectopic bone formation after 5 weeks of implantation. Here, (A–C) denote HAp/col-alginate with BMP; (A), (B), (C), and (D) stand for HE section of the whole implant, immunostaining section with antiosteocalcin, higher magnification, and collagen sponge with BMP, respectively. Here, bone marrow-like tissue was indicated by white arrows. Further, black arrowheads and white arrowheads indicate soft and bone, respectively [64].

Ripamonti et al. conducted spontaneous induction research of bone formation in heterotopic *rectus abdominis* and orthotopic calvarial sites by coral-derived biomimetic matrices of different chemical compositions. The authors conducted a long-term study in the non-human primate *Papio ursinus*. In this methodology, rods (diameter 20 mm × and 7 mm) were implanted in heterotopic *rectus abdominis* sites; discs (diameter 25 mm) were implanted in orthotopic calvarial defects of six adult non-human primates, *P. ursinus.* Fully converted hydroxyapatite replicas sintered at 1100°C were used as heterotopic samples. These fully converted hydroxyapatite replicas were coated with the synthetic peptide P15 known to increase the adhesion of fibroblasts to an organic bovine mineral to further enhance the spontaneous osteoinductive activity. Thereafter, bone induction was evaluated by a histological examination, alkaline phosphatase, and osteocalcin expression, as well as by the expression of BMP-7, GDF-10, and collagen type IV mRNAs at 60, 90, and 365 days. Bone induction occurred in the concavities of the scaffolds matrices at all time points. It was evident of bone marrow formation in the P15-coated and uncoated implants at 365 days. Moreover, resorption of partially converted calcium carbonate/hydroxyapatite and remodeling of the newly formed bone was apparent. The northern blot analyses of samples from heterotopic specimens indicated high levels of expression of BMP-7 and collagen type IV mRNA in all samples at 60 days. Therefore, it was correlating with the induction of the osteoblastic phenotype in invading fibrovascular cells. Expanded bone formation across the different implanted constructs of the orthotopic samples was also observed (**Figure 9**).

The concavities of the biomimetic matrices and the remodeling cycle of the osteogenic primate cortico-cancellous bone stimulate the ripple-like cascade of the induction of bone formation. It is demonstrated for the first time through this study that spontaneous differentiation of bone was induced by partially converted HAp/CC constructs. It was noted that this bone induction was only seen 1 year post-implantation [12].

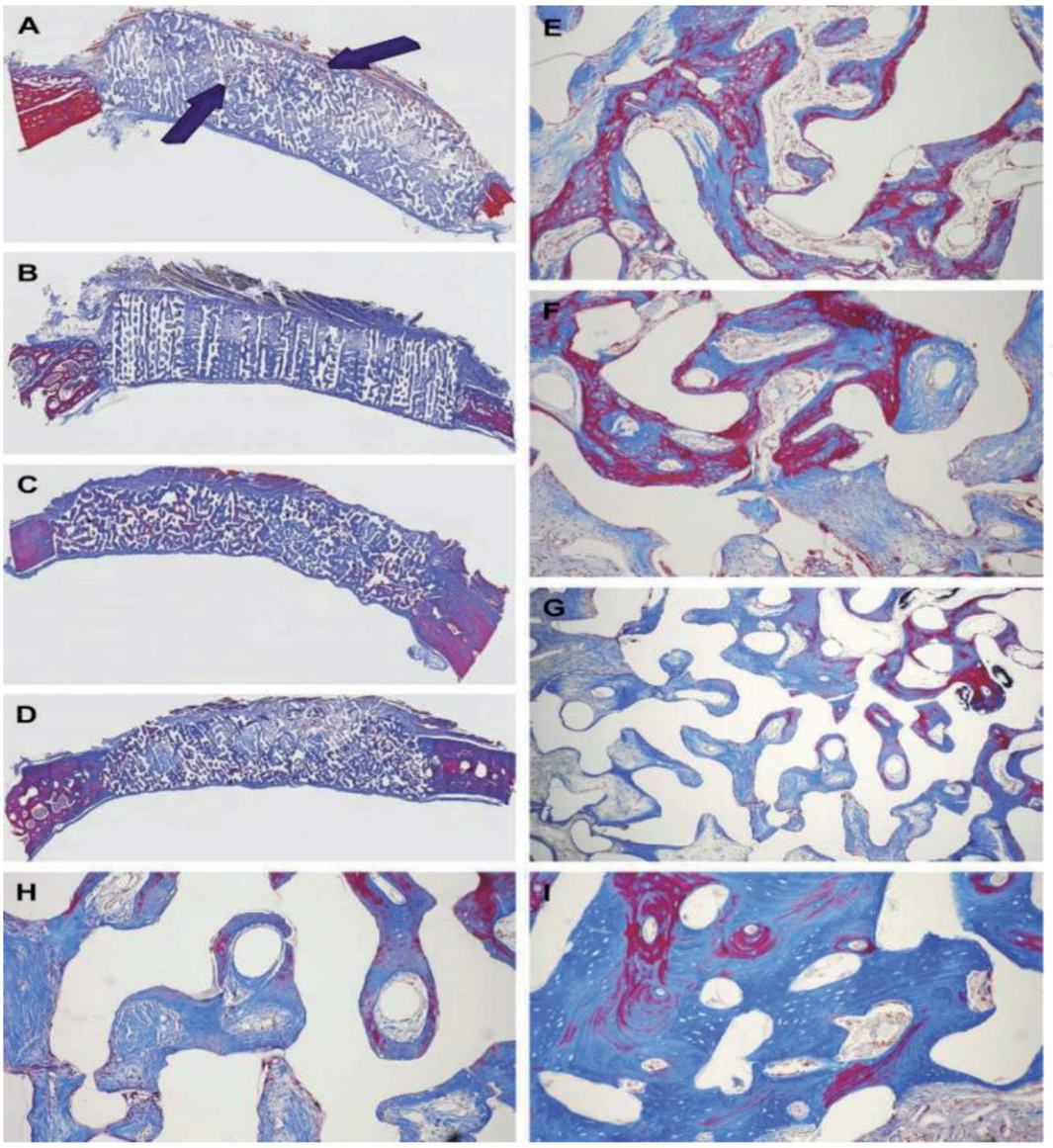


Figure 9.
Demonstration of calvarial incorporation of 13% hydroxyapatite/calcium carbonate paradigms collected on 60 (A, E, F), 90 (B, F, G, H), and 365 days (C, D, and I) after implantation in calvarial defects of Papio ursinus*. Here, (a) stands for islands of newly formed bone (blue arrows) scattered within the internal and central regions of the implanted coral-derived construct; (E and F) stand for the induction of bone formation within the porous spaces of the implanted biomimetic matrices; (B, F, G, and H) stand for induction of bone formation in porous biomimetic constructs harvested 90 days after implantation in calvarial defects. Further, (C, D, and I) denote calvarial constructs harvested on day 365 after implantation showing significant induction of bone formation with solid blocks (I) of newly formed bone [12].*

Ripamonti et al. also fabricated osteoinductive titanium implants for the induction of bone formation. The experimental titanium implants were prepared with a sequence of 36 repetitive concavities. The estimated diameter, depth, and space distance of these concavities was 1600, 800, and 1000 μm, respectively. To prepare edentulous mandibular ridges for later implantation, mandibular molars and premolars were taken out. After a healing period of 7–8 months, in the left and right, edentulized hemi-mandibles planar and geometric hydroxyapatite-coated titanium constructs were entrenched, respectively. In this study, three planar and three geometric implants were implanted in the left and right tibiae, respectively; additionally, planar and geometric constructs were also inserted in the *rectus abdominis* muscle. A total of six animals were euthanized at 30 and 90 days after implantation for this study; one animal was euthanized 5 days after surgery, and the remaining animal was euthanized 31 months after implantation. Undecalcified longitudinal

sections were precision-sawed, ground, and polished to 40–60 μm; all sections were stained with a modified Goldner's trichrome. By the EXAKT precision cutting and grinding system, undecalcified specimen block preparation was accomplished. Histomorphometric analyses of bone in contact (BIC) revealed that there was no difference between the geometric *vs*. planar control implants on day 30; on the other hand, on day 90, the ratio of BIC to surface within the geometric implants was greater than that of the standard planar implants in both mandibular and tibial sites. Further, selected concavities cut into the geometric implants harvested from the *rectus abdominis* muscle 31 months after implantation exhibited the spontaneous induction of bone formation with mineralized bone surfaced by osteoid seams **(Figure 10)**. Therefore, these data in non-human primates indicate that geometrically constructed plasma-sprayed titanium implants are *per se* osteogenic, the concavities providing a unique microenvironment to initiate bone differentiation by induction [65].

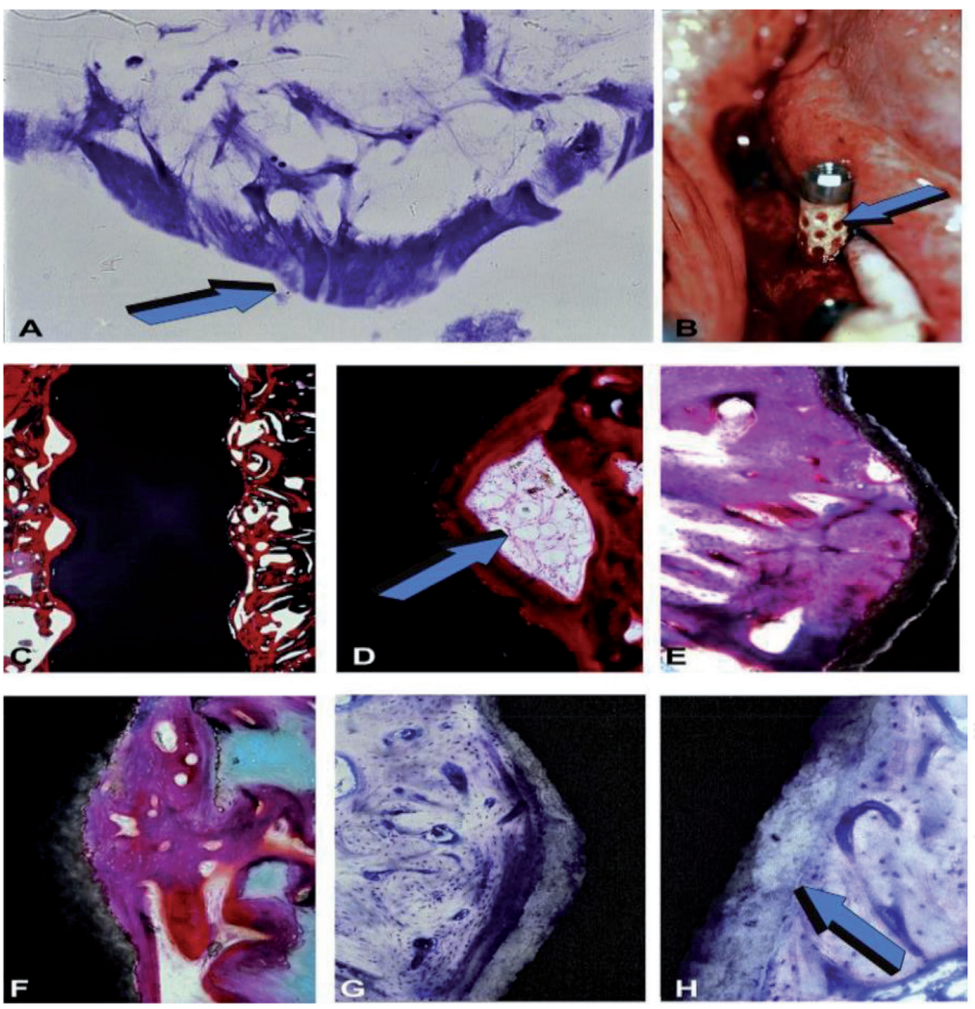


Figure 10.
Tissue evolution, induction, remodeling, and osteointegration within the in vivo *bioreactor of the concavities 90 days after implantation within the edentulized hemi-mandibles of the non-human primate* Papio ursinus. *Here, (A) denotes the instrumental for the preparation of the geometric implants, attachment, orientation, and alignment of MC 3 T3-E1 cells* in vitro *within the geometric cue of the concavity of the coral-derived calcium phosphate macroporous construct. (B) Indicates insertion into the edentulous ridge of the non-human primate* P. ursinus, *the concavities of the* in vivo *bioreactor adsorb plasma and plasma products during the surgical procedure (blue arrow) but not the planar linear inter-concavity spaces. Further, osteointegration along the geometric implant with marrow spaces within the concavity osteointegrated space is denoted by (C) and (D) (blue arrow), whereas mineralized remodeled bone tightly integrated with the hydroxyapatite coating, remodeling, and blending into the highly crystalline hydroxyapatite layer are denoted by E, F, G, H, respectively (H blue arrow) [65].*

In a previous study, porous composite biomaterial of hydroxyapatite (HAp) and periosteal graft was used to repair an induced maxillary bone defect where a defect was created in the premaxillary bone of rats. In this study, four groups were used: (1) those treated with the mucoperiosteal graft from the premaxilla, (2) those treated with HAp combined with a mucoperiosteal graft from the premaxilla, (3) those treated with HAp combined with a periosteal graft from the femur, and (4) those treated with a periosteal graft from the femur. It was revealed from the radiographic evaluation from all groups that no signs of bone formation after 2 weeks were detected but radiolucency was found inside the HAp implants after 16 weeks. It was clear that cell proliferation occurred from the periosteum covering the defect. Moreover, bone tissue formation was detected from the defect margin to inside the defect in all cases. Interestingly, after 8 and 16 weeks of implantation, mature bone was observed around the HAp implants (**Figure 11**). Therefore, it was concluded that the periosteal graft provides reasonable support to the HAp implant, allowing the development of new bone [66].

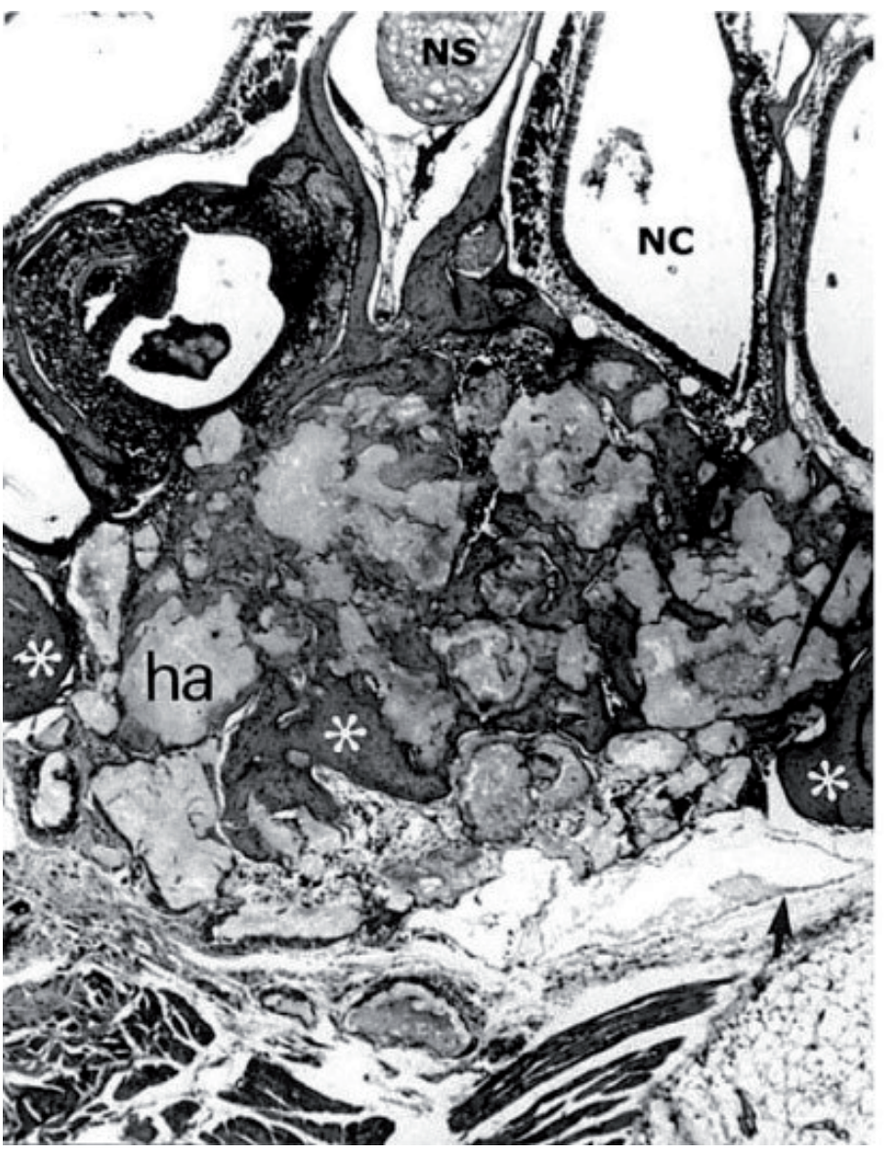


Figure 11.
A histologic frontal section through bone defect covered with mucoperiosteum from the premaxilla combined with HA (group 2). After 16 weeks, the defect in the premaxilla was partially occupied by newly formed bone (white stars) with a mature appearance and by the HA blocks, while there were spaces filled by connective tissue. The mucoperiosteum from the premaxilla remained the HA blocks in the defect (black arrow). (Original magnification 32; hematoxylin-eosin stain).

Composites	Cell culturing or implantation	Period (new tissue formed)
CO3Appatite-Collagen (Okazaki et al.) [67]	Implantation in rat periosteum cranii	21 days (mineralized bone)
PCCA-TCP-Collagen (Du et al.) [68]	Implantation in rat thigh muscle	7 days (connective tissue and capillary vessels)
HA-Collagen (Kikuchi et al.) [69]	Implantation in beagle tibia	54 days (mineralized bone)
HA-Collagen (Itoh et al.) [70]	Implantation in beagle cervical spine	14 days (start of callus formation)
FGMgCO3Ap-Collagen (Yamasaki et al.) [71]	Implantation in rat periosteum cranii	14–28 days (mineralized bone)
HA-Collagen Alginate (Sotome et al.) [64]	Implantation in the rat femur	14 days (mineralized bone)
nHA-Anionic Collagen (Martins and Goissis) [72]	Implantation in rat infraorbital bone	60 days (mineralized bone)
cAP-Collagen (Suh et al.) [73]	Implantation in rabbit skin	98 days (mineralized bone)

Table 2.
In vivo *experiments in bone tissue engineering using different HAp composites.*

Moreover, Wahl and Czernuszka (2006) summarized and compared a few excellent reports of *in vivo* experiments using HAp composite scaffolds and are listed here in **Table 2** [56].

The biodegradable porous scaffolds of HAp synthesized and fabricated by the mentioned methods showed several advantages and disadvantages. The porosity of the HAp scaffolds plays an important role in tissue engineering to control cell functions and to guide the formation of new tissues and organs. Therefore, no matter what the materials are, scaffolds must have sufficient porosity to allow for cellular infiltration and proper cell function [31]. The fabricated pore structures of HAp scaffolds facilitated cell seeding, cell penetration, and distribution in the scaffolds. On the other hand, the bottleneck of the mentioned methods was time-consuming.

4. Conclusion

Recently, bone and cartilage generation by autogenous cell/tissue transplantation has become one of the most promising techniques in orthopedic surgery and biomedical engineering. Several scaffold materials have been investigated for tissue engineering bone and cartilage. Hydroxyapatite (HAp) composite is an eminent one among them. It has been investigated for its clinical viability in various bone defects since the mid-1980s. Synthetic HAp exhibits good properties as a biomaterial, such as biocompatibility, bioactivity, and osteoconductivity. Therefore, it has been widely used as a bone substitute, coating on metallic implants, and scaffold for tissue engineering. HAp along with other biopolymers, ceramics, and metals produced composite scaffolds to enhance the ease of application of tissue engineering. HAp-COL and HAp-COL/HAp composite scaffolds or HAp-CNT nanocomposites for orthopedic implants are synthesized and fabricated through template method, plasma spraying, laser surface alloying, electrophoretic deposition, aerosol deposition, and a specific freeze-drying procedure. Several *in vitro* and *in vivo* experiments conducted worldwide demonstrated and proved the inevitabilities and excellences of HAp composite scaffolds in bone tissue regeneration and engineering.

Acknowledgements

The authors gratefully acknowledge the financial support by The World Academy of Sciences (TWAS) for the Research Grant No. 19-143 RG/CHE/AS_I—FR3240310168. The authors are very much grateful to Mohammad Asaduzzaman, Lecturer, Department of English, Shaheed Police Smrity College, Mirpur 14, Dhaka, Bangladesh.

Conflict of interest

The authors declare no conflict of interest.

Author details

Mohammad Shariful Islam[1*], Mohammad Abdulla-Al-Mamun[2], Alam Khan[3] and Mitsugu Todo[4]

1 Department of Veterinary and Animal Sciences, University of Rajshahi, Rajshahi, Bangladesh

2 Institute of Leather Engineering and Technology, University of Dhaka, Bangladesh

3 Department of Pharmacy, University of Rajshahi, Rajshahi, Bangladesh

4 Research Institute for Applied Mechanics, Kyushu University, Kasuga, Fukuoka, Japan

*Address all correspondence to: msips06@ru.ac.bd

IntechOpen

© 2020 The Author(s). Licensee IntechOpen. This chapter is distributed under the terms of the Creative Commons Attribution License (http://creativecommons.org/licenses/by/3.0), which permits unrestricted use, distribution, and reproduction in any medium, provided the original work is properly cited. CC BY

References

[1] Islam MS et al. Effects of compressive ratio and sintering temperature on mechanical properties of biocompatible collagen/hydroxyapatite composite scaffolds fabricated for bone tissue engineering. Journal of Asian Ceramic Societies. 2019;**7**(2):183-198

[2] Gu Y, Huang W, Rahaman MN, Day DE. Bone regeneration in rat calvarial defects implanted with fibrous scaffolds composed of a mixture of silicate and borate bioactive glasses. Acta Biomaterialia. 2013;**9**:9126-9136

[3] Zhang X et al. Polymer-ceramic spiral structured scaffolds for bone tissue engineering: Effect of hydroxyapatite composition on human fetal osteoblasts. PLoS One. 2014;**9**:85871

[4] Meng J et al. Super-paramagnetic responsive nanofibrous scaffolds under static magnetic field enhance osteogenesis for bone repair in vivo. Science Reports. 2013;**3**:2655

[5] Dubok VA. Bioceramics-yesterday, today, tomorrow. Powder Metallurgy and Metal Ceramics. 2000;**39**:381-394

[6] Jarcho M. Calcium phosphate ceramics as hard tissue prosthetics. Clinical Orthopaedics and Related Research. 1981;**157**:259-278

[7] Tamai N, Myoui A, Tomita T, Nakase T, Tanaka J, Ochi T, et al. Novel hydroxyapatite ceramics with an inter connective porous structure exhibit superior osteoconduction in vivo. Journal of Biomedical Materials Research. 2002;**59A**:110-117

[8] Raquel ZL. Apatites in biological systems. Progress in Crystal Growth and Characterization. 1981;**4**:1-45.6

[9] Posner AS, Betts F. Synthetic amorphous calcium phosphate and its relation to bone mineral structure. Accounts of Chemical Research. 1975;**8**:273-281

[10] LeGeros RZ. Calcium phosphate-based osteoinductive materials. Chemical Reviews. 2008;**108**:4742-4753

[11] Habibovic P, Gbureck U, Doillon CJ, Bassett DC, van Blitterswijk CA, Barralet JE. Osteoconduction and osteoinduction of low-temperature 3D printed bioceramic implants. Biomaterials. 2008;**29**:944-953

[12] Ripamonti U, Crooks J, Khoali L, Roden L. The induction of bone formation by coral-derived calcium carbonate/hydroxyapatite constructs. Biomaterials. 2009;**30**:1428-1439

[13] Ripamonti U, Richter PW, Nilen RWN, Renton L. The induction of bone formation by smart biphasic hydroxyapatite tricalcium phosphate biomimetic matrices in the non-human primate Papio ursinus. Journal of Cellular and Molecular Medicine. 2008;**12**:1-15

[14] Yuan H, Kurashina K, de Bruijn JD, Li Y, de Groot K, Zhang X. A preliminary study on osteoinduction of two kinds of calcium phosphate ceramics. Biomaterials. 1999;**20**:1799-1806

[15] Kattimani VS et al. Hydroxyapatite-past, present, and future in bone regeneration. Bone and Tissue Regeneration Insights. 2016;**7**:9-19. DOI: 10.4137/BTRi.s36138

[16] Hing K, Annaz B, Saeed S, Revell P, Buckland T. Microporosity enhances bioactivity of synthetic bone graft substitutes. Journal of Materials Science. Materials in Medicine. 2005;**16**:467-475

[17] Boyde A, Corsi A, Quarto R, Cancedda R, Bianco P. Osteoconduction

in large macroporous hydroxyapatite ceramic implants: Evidence for a complementary integration and disintegration mechanism. Bone. 1999;**24**:579-589

[18] Hing KA. Bioceramic bone graft substitutes: Influence of porosity and chemistry. Clinical Orthopaedics and Related Research. 2005;**2**:184-199

[19] Hench LL, Wilson J. Surface-active biomaterials. Science. 1984;**226**:630-706

[20] Hulbert SF, Young FA, Mathews RS, Klawitter JJ, Talbert CD, Stelling FH. Potential of ceramic materials as permanently implantable skeletal prostheses. Journal of Biomedical Materials Research. Part A. 1970;**4**:433-456

[21] Mobasherpour I, Hashjin MS, Toosi SSR, Kamachali RD. Effect of the addition ZrO2-Al2O3 on nanocrystalline hydroxyapatite bending strength and fracture toughness. Ceramics International. 2009;**35**:1569-1574

[22] Thomson RC, Wake MC, Yaszemski MJ, Mikos AG. Biodegradable polymer scaffolds to regenerate organs. Advances in Polymer Science. 1997;**122**:245-274

[23] Persidis A. Tissue engineering. Nature Biotechnology. 1999;**17**(5):508-510

[24] Service RF. Tissue engineers build new bone. Science. 2000;**289**(5484):1498-1500

[25] Petite H, Viateau V, Bensaid W, Meunier A, de Pollak C, Bourguignon M, et al. Tissue engineered bone regeneration. Nature Biotechnology. 2000;**18**(9):959-963

[26] Azevedo MC, Reis RL, Claase MB, Grijpma DW, Feijen J. Development and properties of polycaprolactone/ hydroxyapatite composite biomaterials. Journal of Materials Science. Materials in Medicine. 2003;**14**:103-107

[27] Guarino V, Causa F, Netti PA, Ciapetti G, Pagani S, Martini D, et al. The role of hydroxyapatite as solid signal on performance of PCL porous scaffolds for bone tissue regeneration. Journal of Biomedical Materials Research Part B: Applied Biomaterials. 2008;**86**:548-557

[28] Kim HW, Knowles JC, Kim HE. Hydroxyapatite/poly(εcaprolactone) composite coatings on hydroxyapatite porous bone scaffold for drug delivery. Biomaterials. 2004;**25**:1279-1287

[29] Mourinño V, Boccaccini AR. Bone tissue engineering therapeutics-controlled drug delivery in three dimensional scaffolds. Journal of the Royal Society, Interface. 2010;**7**: 209-227

[30] Kim SS et al. Poly(lactide-co-glycolide)/hydroxyapatite composite scaffolds for bone tissue engineering. Biomaterials. 2006;**27**:1399-1409

[31] Islam MS, Todo M. Effects of sintering temperature on the compressive mechanical properties of collagen/hydroxyapatite composite scaffolds for bone tissue engineering. Materials Letters. 2016;**173**:231-234

[32] Balani K, Zhang T, Karakoti A, Li WZ, Seal S, Agarwal A. In situ carbon nanotube reinforcements in a plasma-sprayed aluminum oxide nanocomposite coating. Acta Materialia. 2008;**56**:571-579

[33] Ma RZ, Wu J, Wei BQ, Liang J, Wu DH. Processing and properties of carbon nanotubes-nano-SiC ceramic. Journal of Materials Science. 1998;**33**:5243-5246

[34] Lahiri D, Singh V, Keshri AK, Seal S, Agarwal A. Carbon nanotube toughened hydroxyapatite by spark plasma

sintering: Microstructural evolution and multiscale tribological properties. Carbon N Y. 2010;**48**:3103-3120

[35] Cheng GJ, Pirzada D, Cai M, Mohanty P, Bandyopadhyay A. Bioceramic coating of hydroxyapatite on titanium substrate with Nd-YAG laser. Materials Science and Engineering: C. 2005;**25**:541-547

[36] Singh I, Kaya C, Shaffer MSP, Thomas BC, Boccaccini AR. Bioactive ceramic coatings containing carbon nanotubes on metallic substrates by electrophoretic deposition. Journal of Materials Science. 2006;**41**:8144-8151

[37] Hahn B, Lee J, Park D, et al. Mechanical and in vitro biological performances of hydroxyapatite–carbon nanotube composite coatings deposited on Ti by aerosol deposition. Acta Biomaterialia. 2009;**5**:3205-3214

[38] Li A, Sun K, Dong W, Zhao D. Mechanical properties, microstructure and histocompatibility of MWCNTs/HAp biocomposites. Materials Letters. 2007;**61**:1839-1844

[39] Li H, Zhao N, Liu Y, et al. Fabrication and properties of carbon nanotubes reinforced Fe/hydroxyapatite composites by in situ chemical vapor deposition. Composites Part A: Applied Science and Manufacturing. 2008;**39**:1128-1132

[40] Omori M, Okubo A, Otsubo M, Hashida T, Tohji K. Consolidation of multiwalled carbon nanotube and hydroxyapatite coating by the spark plasma system (SPS). Key Engineering Materials. 2004;**25**(4-256):395-398

[41] Xu JL, Khor KA, Sui JJ, Chen WN. Preparation and characterization of a novel hydroxyapatite/carbon nanotubes composite and its interaction with osteoblastlike cells. Materials Science and Engineering: C. 2009;**29**:44-49

[42] Phanny Y. Development and characterization of polymer/bioceramic composite porous biomaterials for bone tissue engineering [thesis]. Japan: Kyushu University; 2014

[43] Catherine G, Charles JD. Facilitating tissue infiltration and angiogenesis in a tubular collagen scaffold. Journal of Biomedical Materials Research Part A. 2009;**93**:615-624. DOI: 10.1002/jbm.a.32568

[44] Heinemann C, Heinemann S, Bernhardt A, Worch H, Hanke T. Novel textile chitosan scaffolds promote spreading, proliferation, and differentiation of osteoblasts. Biomacromolecules. 2008;**9**:2913-2920. DOI: 10.1021/bm800693d

[45] Girotto D, Urbani S, Brun P, Renier D, Barbucci R, Abatangelo G. Tissue-specific gene expression in chondrocytes grown on three-dimensional hyaluronic acid scaffolds. Biomaterials. 2003;**24**:3265-3275. DOI: 10.1016/S0142-9612(03)00160-1

[46] Park JE, Todo M. Development and characterization of reinforced poly(l-lactide) scaffolds for bone tissue engineering. Journal of Materials Science. Materials in Medicine. 2011;**22**:1171-1182. DOI: 10.1007/s10856-011-4289-4

[47] Joshua RP, Andrew H, Ketul CP. Biodegradable poly(ε-caprolactone) nanowires for bone tissue engineering applications. Biomaterials. 2009;**30**:780-788. DOI: 10.1016/j.biomaterials.2008.10.022

[48] Lohan A, Marzahn U, El Sayed K, Haisch A, Kohl B, Müller RD, et al. In vitro and in vivo neo-cartilage formation by heterotopic chondrocytes seeded on PGA scaffolds. Histochemistry and Cell Biology. 2011;**136**:57-69. DOI: 10.1007/s00418-011-0822-2

[49] Wiria FE, Chua CK, Leong KF, Quah ZY, Chandrasekaran M, Lee MW. Improved biocomposite development of poly(vinyl alcohol) and hydroxyapatite for tissue engineering scaffold fabrication using selective laser sintering. Journal of Materials Science. Materials in Medicine. 2008;**19**:989-996. DOI: 10.1007/s10856-007-3176-5

[50] Zhang X, Guo YLi DX, Wang R, Fan HS, Xiao YM, Zhang L, et al. The effect of loading icariin on biocompatibility and bioactivity of porous β-TCP ceramic. Journal of Materials Science: Materials in Medicine. 2011;**22**:371-379. DOI: 10.1007/s10856-010-4198-y

[51] Udoh KMunar ML, Maruta M, Matsuya S, Ishikawa K. Effects of sintering temperature on physical and compositional properties of α-tricalcium phosphate foam. Dental Materials Journal. 2010;**29**:154-159

[52] Arpornmaeklong P, Pripatnanont P, Suwatwirote N. Properties of chitosan-collagen sponges and osteogenic differentiation of rat-bone-marrow stromal cells. International Journal of Oral and Maxillofacial Surgery. 2008;**37**:357-366. DOI: 10.1016/j.ijom.2007.11.014

[53] Akkouch A, Zhang Z, Rouabhia M. A novel collagen/hydroxyapatite/poly(lactide-co-ε-caprolactone) biodegradable and bioactive 3D porous scaffold for bone regeneration. Journal of Biomedical Materials Research Part A. 2011;**96**:693-704. DOI: 10.1002/jbm.a.33033

[54] Salerno A, Zeppetelli S, Di Maio E, Iannace S. Processing/structure/property relationship of multi-scaled PCL and PCL-HA composite scaffolds prepared via gas foaming and NaCl reverse templating. Biotechnology and Bioengineering. 2011;**108**:963-976. DOI: 10.1002/bit.23018

[55] Hiraoka Y, Kimura Y, Ueda H, Tabata Y. Fabrication and biocompatibility of collagen sponge reinforced with poly(glycolic acid) fiber. Tissue Engineering. 2003;**9**:1101-1112. DOI: 10.1089/10763270360728017

[56] Wahl DA, Czernuszka JT. Collagen-hydroxyapatite composites for hard tissue repair. European Cells & Materials. 2006;**11**:43-56

[57] Du C, Cui FZ, Zhu XD, de Groot K. Three dimensional nano-HAp/collagen matrix loading with osteogenic cells in organ culture. Journal of Biomedical Materials Research. 1999;**44**:407-415

[58] Clarke KI, Graves SE, Wong ATC, Triffitt JT, Francis MJO, Czernuszka JT. Investigation into the formation and mechanical-properties of a bioactive material based on collagen and calcium-phosphate. Journal of Materials Science. Materials in Medicine. 1993;**4**:107-110

[59] Wu TJ, Huang HH, Lan CW, Lin CH, Hsu FY, Wang YJ. Studies on the microspheres comprised of reconstituted collagen and hydroxyapatite. Biomaterials. 2004;**25**:651-658

[60] Wang X, Grogan SP, Rieser F, Winkelmann V, Maquet V, Berge ML, et al. Tissue engineering of biphasic cartilage constructs using various biodegradable scaffolds: An in vitro study. Biomaterials. 2004;**25**:3681-3688

[61] Rovira A, Amedee J, Bareille R, Rabaud M. Colonization of a calcium phosphate elastin-solubilized peptide-collagen composite material by human osteoblasts. Biomaterials. 1996;**17**:1535-1540

[62] Cai L, Wang Q, Gu C, Wu J, Wang J, Kang N, et al. Vascular and micro-environmental influences on MSC-coral hydroxyapatite construct-based bone tissue engineering. Biomaterials. 2011;**32**:8497-8505

[63] Kikuchi M, Itoh S, Ichinose S, Shinomiya K, Tanaka J. Self-organization mechanism in a bone-like hydroxyapatite/collagen nanocomposite synthesized in vitro and its biological reaction in vivo. Biomaterials. 2001;**22**:1705-1711

[64] Sotome S, Uemura T, Kikuchi M, Chen J, Itoh S, Tanaka J, et al. Synthesis and in vivo evaluation of a novel hydroxyapatite/collagenalginate as a bone filler and a drug delivery carrier of bone morphogenetic protein. Materials Science and Engineering: C. 2004;**24**:341-347

[65] Ripamonti U, Roden LC, Renton LF. Osteoinductive hydroxyapatite-coated titanium implants. Biomaterials. 2012;**33**(15):3813-3823

[66] Caria PH, Kawachi EY, Bertran CA, Camilli JA. Biological assessment porousimplant hydroxyapatite of combined with periosteal grafting in maxillary defects. Journal of Oral and Maxillofacial Surgery. 2007;**65**:847-854

[67] Okazaki M, Ohmae H, Takahashi J, Kimura H, Sakuda M. Insolubilized properties of UV-irradiated C03 apatite-collagen composites. Biomaterials. 1990;**11**:568-572

[68] Du C, Cui FZ, Zhang W, Feng QL, Zhu XD, de Groot K. Formation of calcium phosphate/collagen composites through mineralization of collagen matrix. Journal of Biomedical Materials Research. 2000;**50**:518-527

[69] Kikuchi M, Itoh S, Ichinose S, Shinomiya K, Tanaka J. Self-organization mechanism in a bone-like hydroxyapatite/collagen nanocomposite synthesized in vitro and its biological reaction in vivo. Biomaterials. 2001;**22**:1705-1711

[70] Itoh S, Kikuchi M, Koyama Y, Takakuda K, Shinomiya K, Tanaka J. Development of an artificial vertebral body using a novel biomaterial, hydroxyapatite/collagen composite. Biomaterials. 2002;**23**:3919-3926

[71] Yamasaki Y, Yoshida Y, Okazaki M, Shimazu A, Kubo T, Akagawa Y, et al. Action of FGMgCO3Apcollagen composite in promoting bone formation. Biomaterials. 2003;**24**:4913-4920

[72] Martins VCA, Goissis G. Nonstoichiometric hydroxyapatite: Anionic collagen composite as a support for the double sustained release of gentamicin and norfloxacin/ciprofloxacin. Artificial Organs. 2000;**24**:224-230

[73] Suh H, Han D-W, Park J-C, Lee DH, Lee WS, Han CD. A bone replaceable artificial bone substitute: Osteoinduction by combining with bone inducing agent. Artificial Organs. 2001;**25**:459-466